

CNS研究会2006

Jan. 28, 2006

Review of continuum shell model and more

K. Kato

Hokkaido Univ

Continuum shell model (CSM) : long history

C. Mahaux and H. Weidenmüller,

Shell Model Approaches to Nuclear Reactions

(North-Holland, Amsterdam, 1969).

Over the past two decades, a great raise in the number of known unstable nuclei has reinforced the important role of the continuum shell model in order to give microscopic descriptions of weakly bound nuclear systems far from the stability valley.

Recent review articles:

I. Rotter; Rep. Prog. Phys. 54, 635 (1991).

J. Okolowicz, M. Ploszajczak, and I. Rotter,
Phys. Rep. 374, 271 (2003).

However, it is not an easy task to treat the unbound states in the usual frameworks with the single-particle products in which the single particle description deals separately and in different manners with bound and scattering single-particle states.

Recently, a great progress in the continuum shell model has been made by the unified description of single-particle basis wave functions as mentioned below. This kind of continuum shell model is the so-called **Gamow shell model (GSM)** which has been successfully applied to weakly bound states and resonances in light unstable nuclei.

- A. 1) R. Id Beatan, R.J. Liotta, N. Sandulescu and T. Vertse, Phys. Rev. Lett. 89, 042501 (2002).
- 2) R. Id Betan, R. J. Liotta, N. Sandulescu, and T. Vertse, Phys. Rev. C 67, 014322 (2003).
- 3) R. Id Betan, R. J. Liotta, N. Sandulescu, and T. Vertse, Phys. Lett. B 584, 48 (2004).
- B. 1) N. Michel, W. Nazarewicz, M. Ploszajczak, and K. Bennaceur, Phys. Rev. Lett. 89, 042502 (2002).
- 2) N. Michel, W. Nazarewicz, M. Ploszajczak, and J. Okolowicz, Phys. Rev. C 67, 054311 (2003).
- C. 1) G. Hagen, J. S. Vaagen, and M. Hjorth-Jensen, J. Phys. A:Math. Gen. 37, 8991 (2004).
- 2) G. Hagen, M. Hjorth-Jensen and J. S. Vaagen, Phys. Rev. C 71, 044314 (2005).

Gamow Shell Model

In GSM, the separation of single-particle resonances from the ordinary scattering continuum states has been carried out by modifying the branch cut into a contour L on the complex momentum k or the energy ε_k plane.

Single particle states

Hamiltonian: $H_0 = t + V_0$

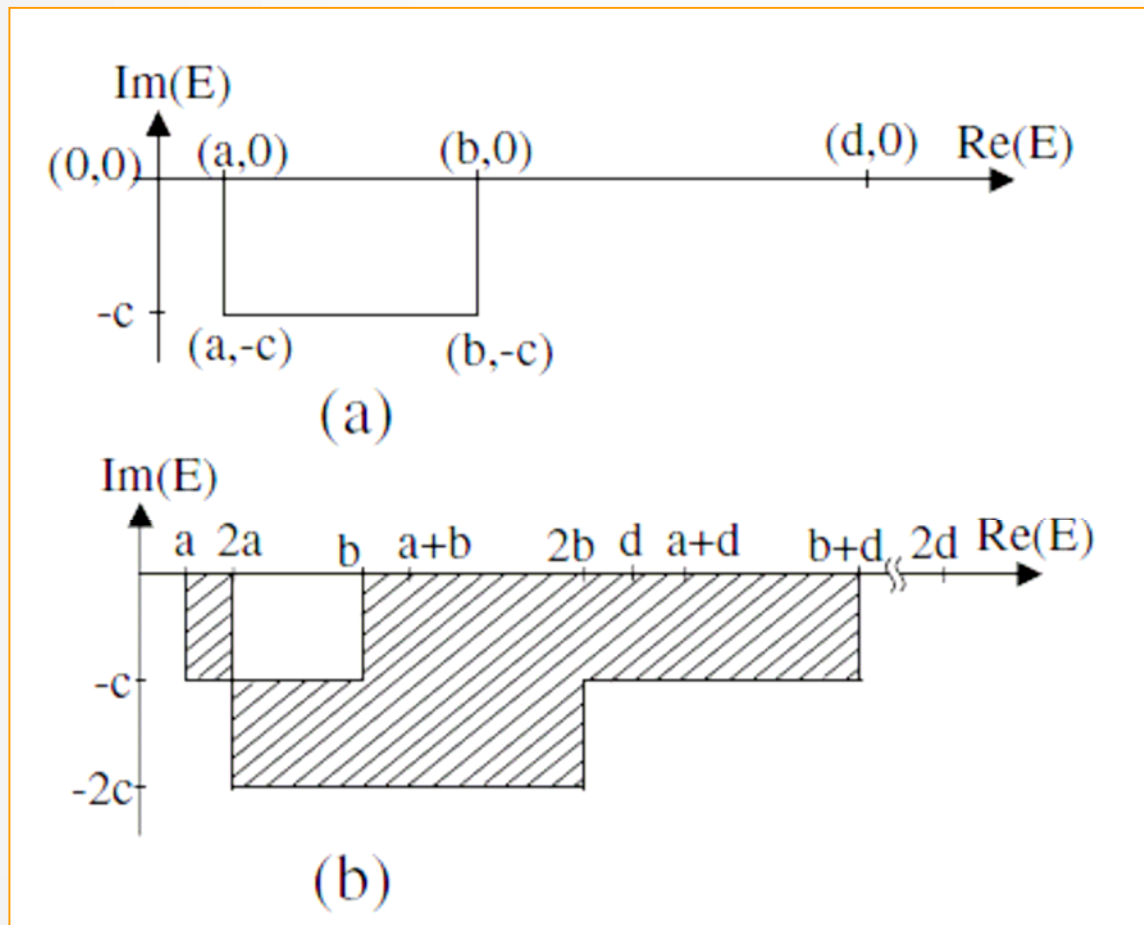
V_0 ; (Woods-Saxon potential) + (l•s force)

$$\frac{\hbar^2}{2\mu} k^2 \psi_{nl}(k) + \frac{2}{\pi} \int_0^\infty dq q^2 V_l(k, q) \psi_{nl}(q) = E_{nl} \psi_{nl}(k).$$

Bound states, Resonant states : **discrete eigenstates**

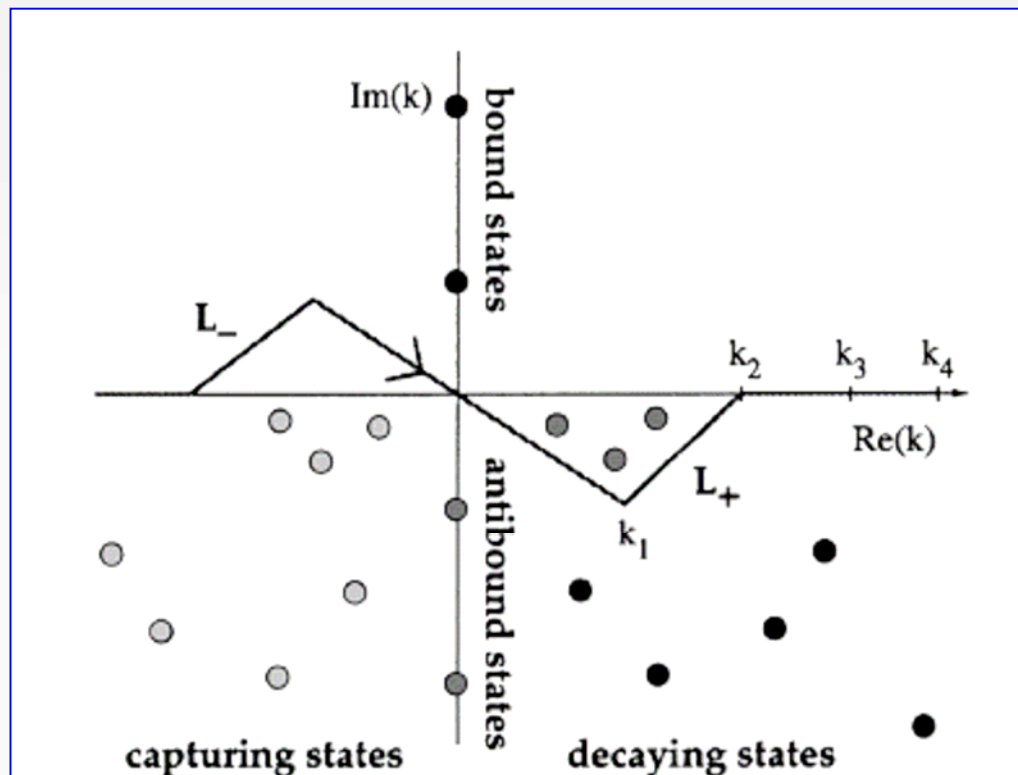
Continuum states ; **Contour L**

Contour L

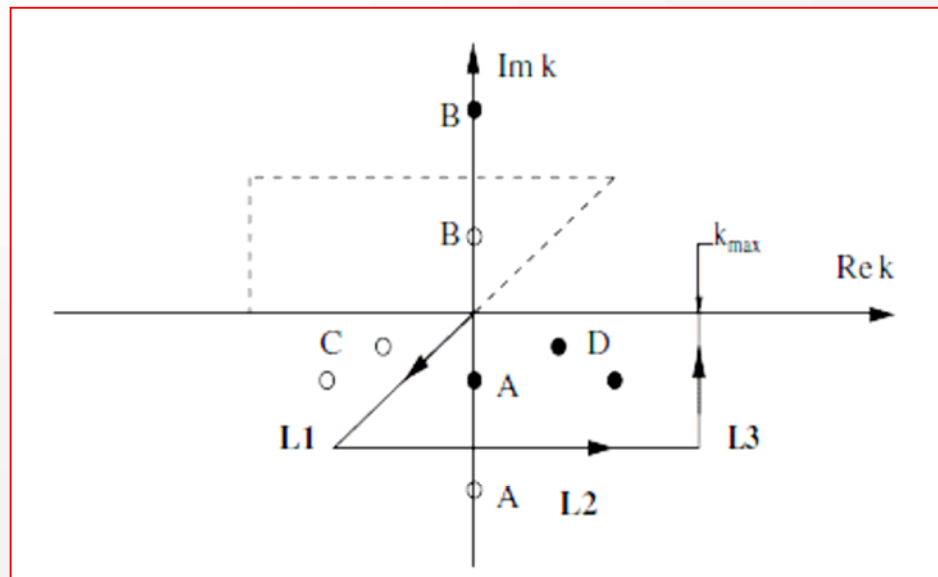
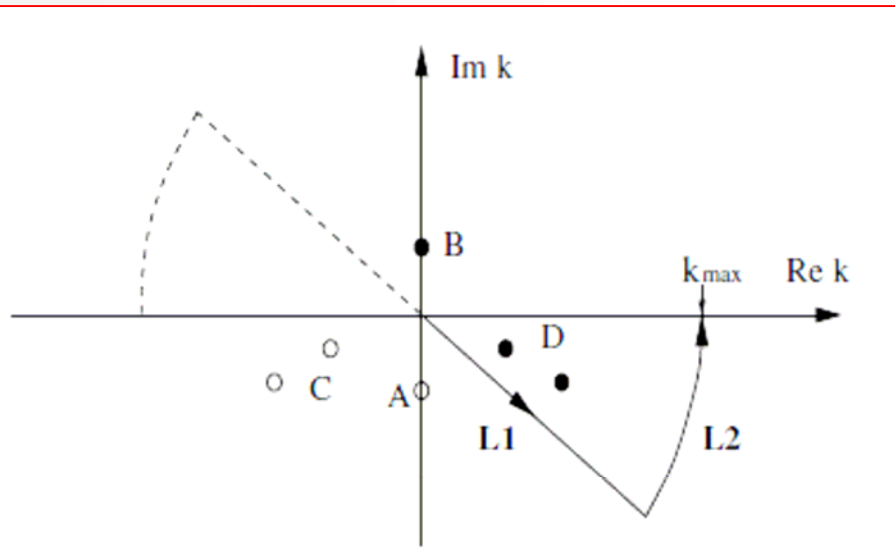


Ref. A-1)

Ref. B-1)



Ref. C-1)



Extended Completeness relation

$$1 = \sum_B |\phi_B\rangle\langle\tilde{\phi}_B| + \int_S |\phi_S\rangle\langle\tilde{\phi}_S|$$

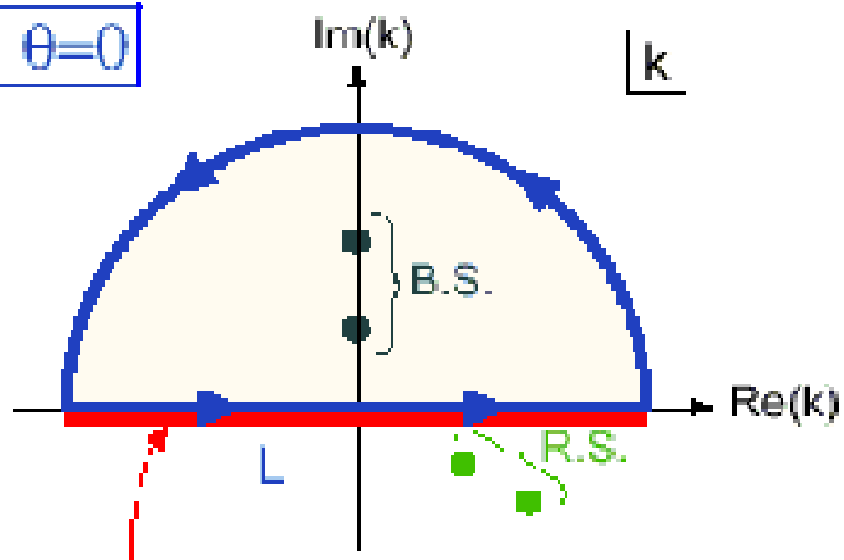


$$1 = \sum_B |\phi_B\rangle\langle\tilde{\phi}_B| + \sum_R |\phi_R\rangle\langle\tilde{\phi}_R| + \int_C |\phi_C\rangle\langle\tilde{\phi}_C|$$

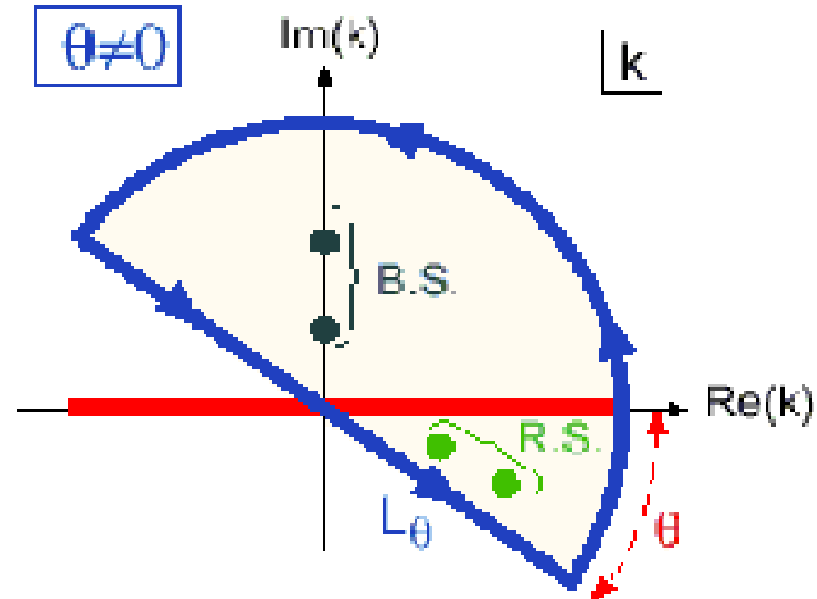
T. Berggren, Nucl. Phys. A109 (1968), 265

T. Myo, A. Ohnishi and K. Kato, Prog. Theor. Phys. 99 (1998), 801

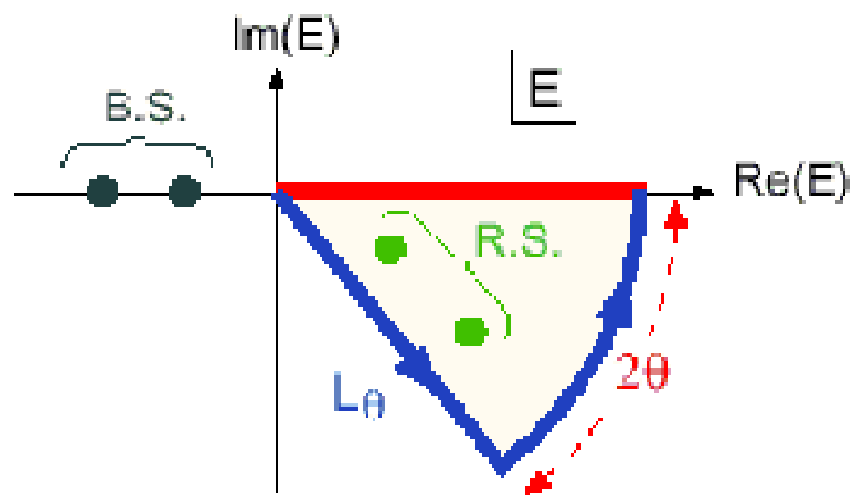
$\theta=0$



$\theta \neq 0$



scattering states



Discretization of continuum states

In practical applications, one has to discretize the integral

$$\int_{L_+} |u_k\rangle\langle\tilde{u}_k| dk \approx \sum_{i=1}^{N_d} |u_i\rangle\langle\tilde{u}_i|$$

where $u_i(r) = \sqrt{\Delta_{k_i}} u_{k_i}(r)$ and Δ_{k_i} is the discretization step.

TABLE V. Convergence of energies corresponding to the states labeled $(1d_{3/2})^2$ in Fig. 7 as a function of the number of Gaussian points n_g . The value $n_g=0$ corresponds to the case where only bound states and Gamow resonances are included in the basis. The columns are labeled by the strength G_α ($\times 10^4$, in MeV).

n_g	4	20	24	28
0	(2.640, -0.896)	(3.299, -0.607)	(3.275, -0.858)	(3.227, -0.975)
10	(2.63416, -0.89697)	(2.13004, -0.42801)	(1.79169, -0.50527)	(1.360, -0.82097)
50	(2.63448, -0.89643)	(2.05694, -0.39779)	(1.70880, -0.43585)	(1.24293, -0.68603)
100	(2.63349, -0.89643)	(2.05889, -0.40198)	(1.67618, -0.44027)	(1.23509, -0.68299)
150	(2.63349, -0.89643)	(2.05889, -0.40198)	(1.67618, -0.44027)	(1.23509, -0.68299)

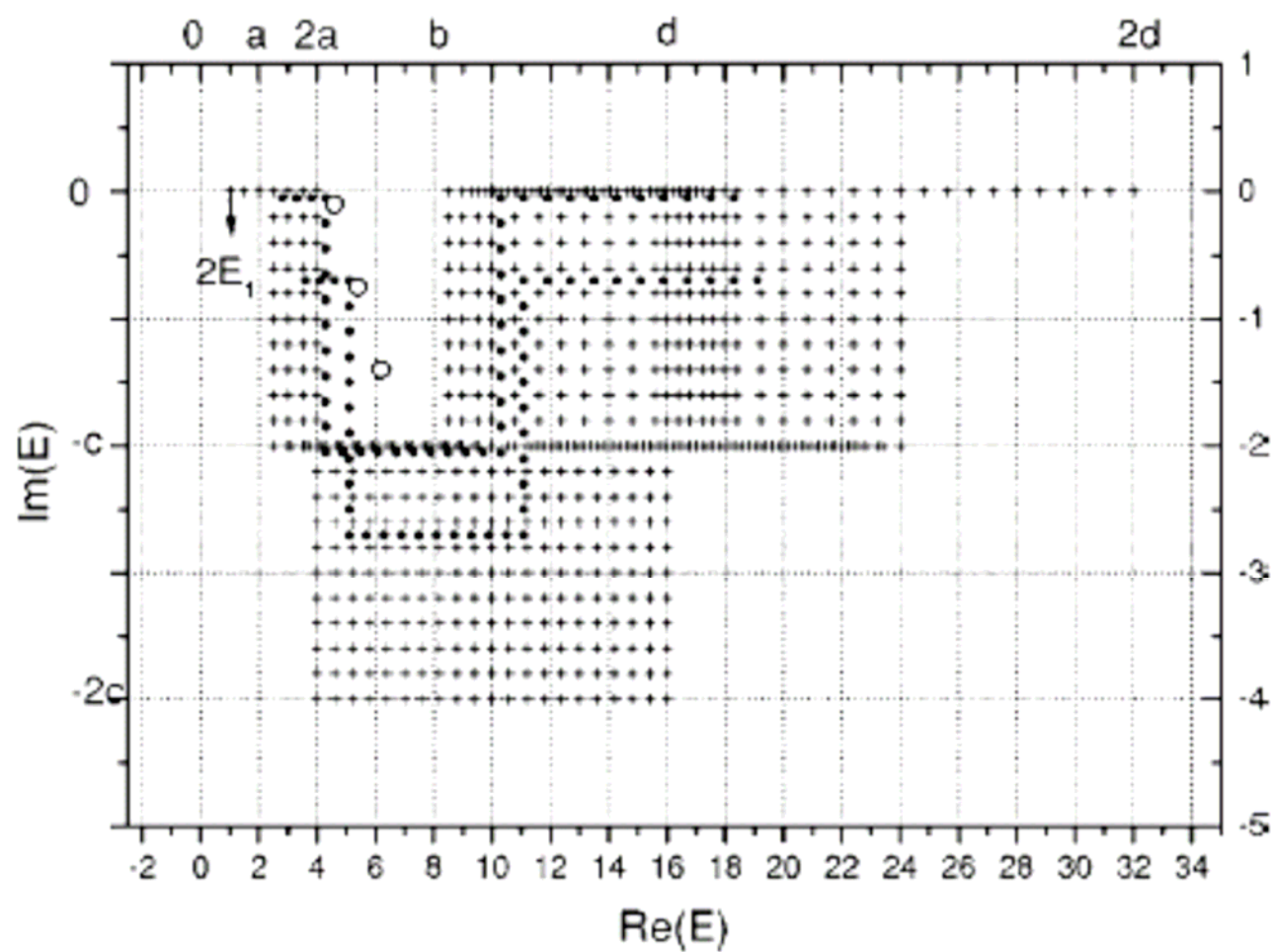


TABLE III. Convergence of the 0_1^+ bound state energy in ${}^6\text{He}$ in terms of the number of integration points N_R and N_T along the rotated C_R and the translated part C_T of the contour, respectively. The number N_{2p} gives the dimension of the two-particle antisymmetrized basis. Only $p_{3/2}$ single-particle orbits are included. Energies are in MeV.

N_R	N_T	N_{2p}	$\text{Re}[E]$	$\text{Im}[E]$
12	12	300	-0.980067	-0.000759
20	20	820	-0.979508	0.000000
25	25	1275	-0.979509	0.000000

TABLE VII. Same as table V, but for the 2_1^+ and 2_2^+ resonance energies.

N_R	N_T	N_{2p}	$J^\pi = 2_1^+$		$J^\pi = 2_2^+$	
			$\text{Re}[E]$	$\text{Im}[E]$	$\text{Re}[E]$	$\text{Im}[E]$
12	12	876	1.149842	-0.203052	2.372295	-2.122474
20	20	2420	1.150527	-0.203060	2.372818	-2.123253
25	25	3775	1.150527	-0.203060	2.372817	-2.123254

Matrix elements of resonant states

1) Ya.B. Zel'dovich, Sov. Phys. JETP 12 (1961), 542

On the Theory of Unstable States

2) Noboru Hokkyo; Prog. Theor. Phys. 33 (1965), 1116.

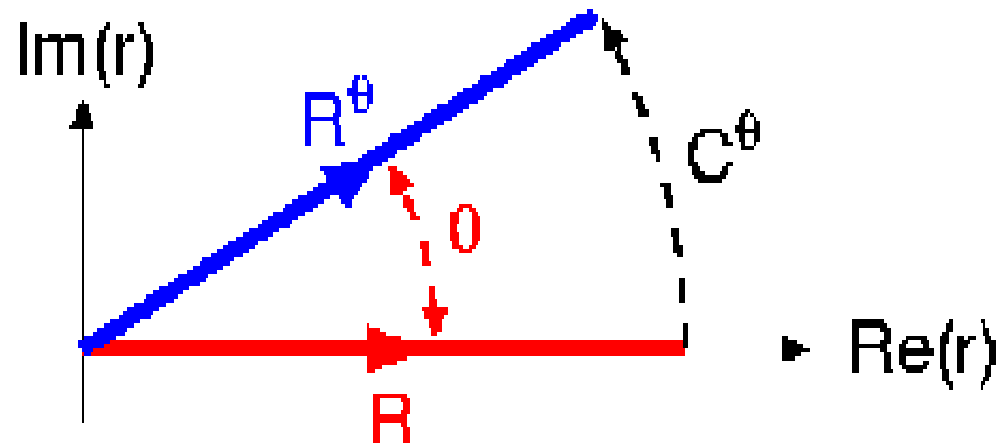
A Remark on the Norm of the Unstable State

—— A role of Adjoint Wave Function in Non-Self-Adjoint Quantum Systems ——

3) B. Gyarmati and T. Vertse; Nucl. Phys. A160 (1971), 523.

On the Normalization of Gamow Functions

- Matrix elements of resonances



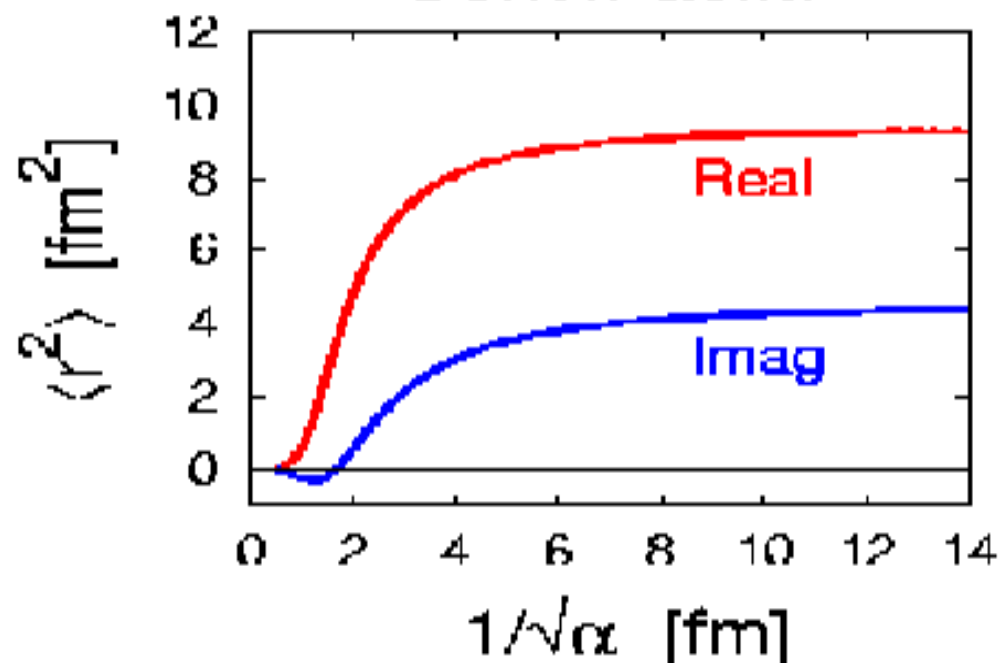
$$\langle \bar{\Phi}_1 | \hat{O} | \Phi_2 \rangle \quad (\text{Conv. Fac. Method})$$

$$= \lim_{\alpha \rightarrow 0} \int_R dr \cdot e^{-\alpha r^2} \cdot \bar{\Phi}_1^* \hat{O} \Phi_2$$

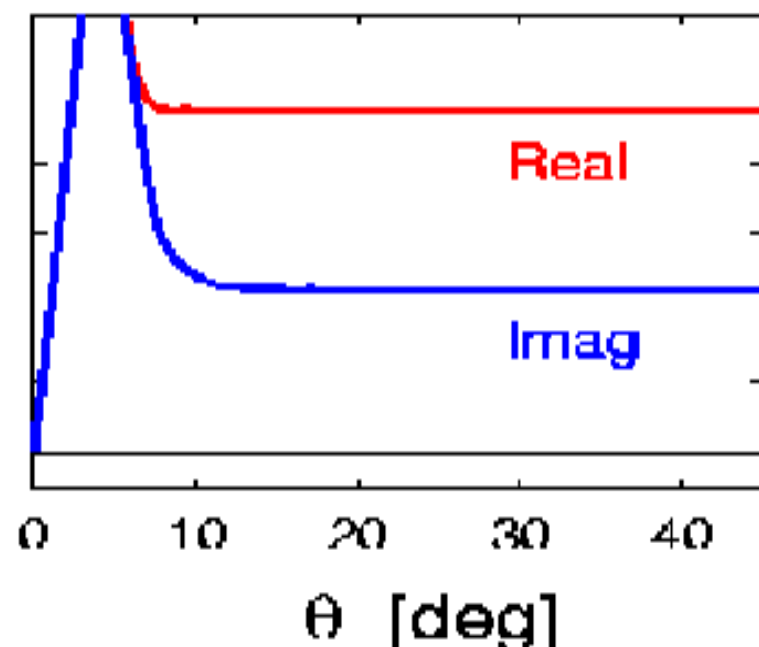
↓

$$= \int_{R^\theta} dr_\theta \cdot \bar{\Phi}_1^{*\theta} \hat{O}^\theta \Phi_2^\theta = \langle \bar{\Phi}_1^\theta | \hat{O}^\theta | \Phi_2^\theta \rangle. \quad (\text{CSM})$$

Conv.Fac.M



C.S.M



[Ref]: W.J.Romo, NPA116(1968),617.

N. Hokkyo, PTP33(1965)1116.

B.Gyarmati, T.Vertse, NPA160(1971)523.

M.Homma, T.Myo, K.Katō, PTP97(1997),561.

In the same way as the standard shell model in a complete discrete basis, for example, that of the harmonic oscillator potential, a N -body Slater determinant Ψ_α is given by the product of N single-particle wave functions as

$$\Psi_\alpha \sim \mathcal{A}\{\psi_{n_1}(r_1) \otimes \psi_{n_2}(r_2) \otimes \cdots \otimes \psi_{n_N}(r_N)\},$$

where the suffix α is an abbreviation of the set of quantum number of the N -body system and n_i describes the single-particle basis $\{nlj; rlj; slj\}$.

The Hamiltonian of GSM is given by one-body and two-body operators, and its concrete forms have been discussed: a separable type [A], a phenomenological force [B] and an effective force derived from the realistic force [C] have been tried as the two-body interaction.

Using GSM, Michel *et al.*: [B] calculated two-particle and many-particle resonances in He-isotopes and O-isotopes.

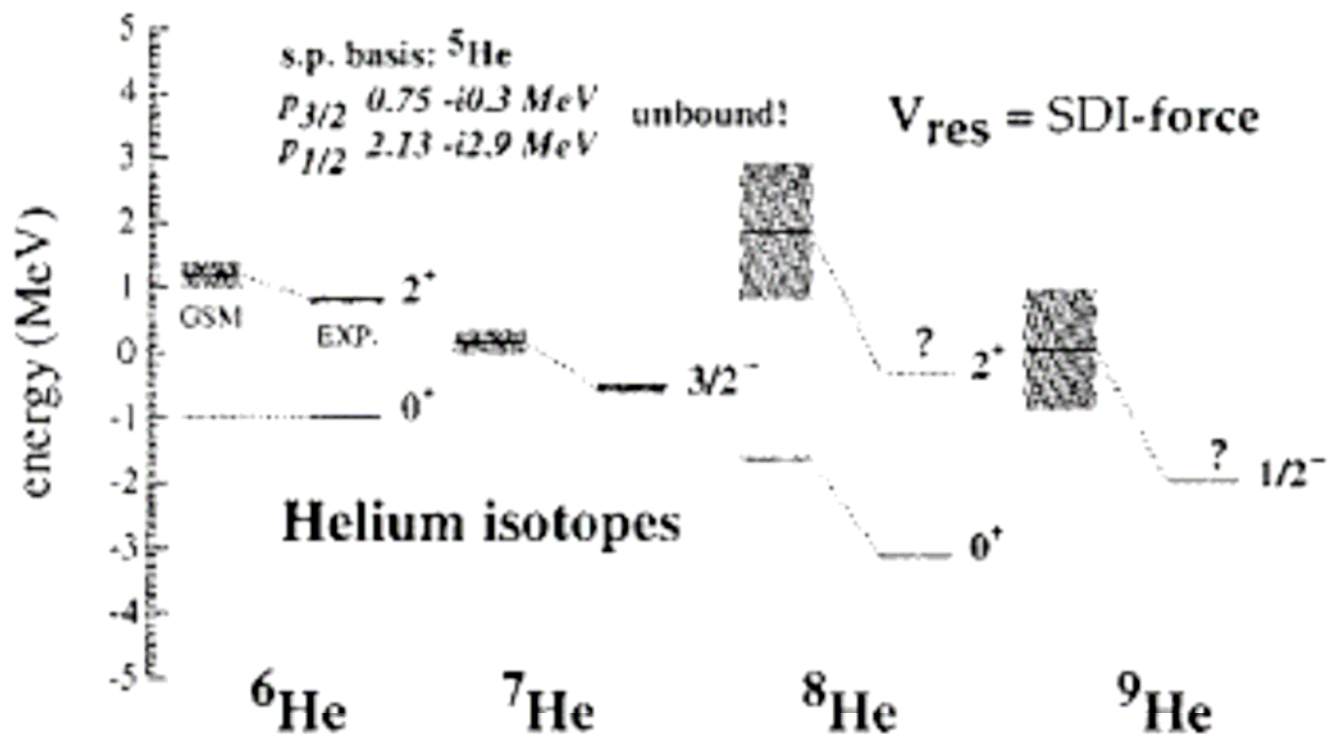


FIG. 19. Experimental (EXP) and predicted (GSM) binding energies of $^6\text{-}^9\text{He}$ as well as energies of $J^\pi = 2^+$ states in $^6,8\text{He}$. The resonance widths are indicated by shading. The energies are given with respect to the core of ^4He .

Nucleus	Configuration	c^2
${}^6\text{He}$	$0p_{3/2}^2$	$0.870 - i0.736$
	$0p_{3/2}^2$	$0.007 - i0.076$
	$L_+^{(1)}$	$0.271 + i0.752$
	$L_+^{(2)}$	$-0.147 + i0.060$
${}^7\text{He}$	$0p_{3/2}^3$	$1.110 - i0.879$
	$0p_{3/2}^2 0p_{1/2}$	$0.006 - i0.029$
	$0p_{3/2} 0p_{1/2}^2$	$0.022 - i0.042$
	$L_+^{(1)}$	$0.050 + i0.951$
	$L_+^{(2)}$	$-0.185 + i0.008$
${}^8\text{He}$	$L_+^{(3)}$	$-0.002 - i0.009$
	$0p_{3/2}^4$	$0.296 - i1.323$
	$0p_{3/2}^2 0p_{1/2}^2$	$-0.060 - i0.158$
	$L_+^{(1)}$	$1.596 + i1.066$
	$L_+^{(2)}$	$-0.728 + i0.630$
	$L_+^{(3)}$	$-0.125 - i0.204$
${}^9\text{He}$	$L_+^{(4)}$	$0.020 - i0.012$
	$0p_{3/2}^4 0p_{1/2}$	$0.180 - i1.328$
	$L_+^{(1)}$	$1.596 + i0.734$
	$L_+^{(2)}$	$-0.584 + i0.801$
	$L_+^{(3)}$	$-0.217 - i0.193$
	$L_+^{(4)}$	$0.025 - i0.034$

Core	V_0 (MeV)	r_0 (fm)	a (fm)	V_{so} (MeV)
^{78}Ni (neutrons)	40	1.27	0.67	21.43
^{100}Sn (protons)	58.5	1.19	0.75	15

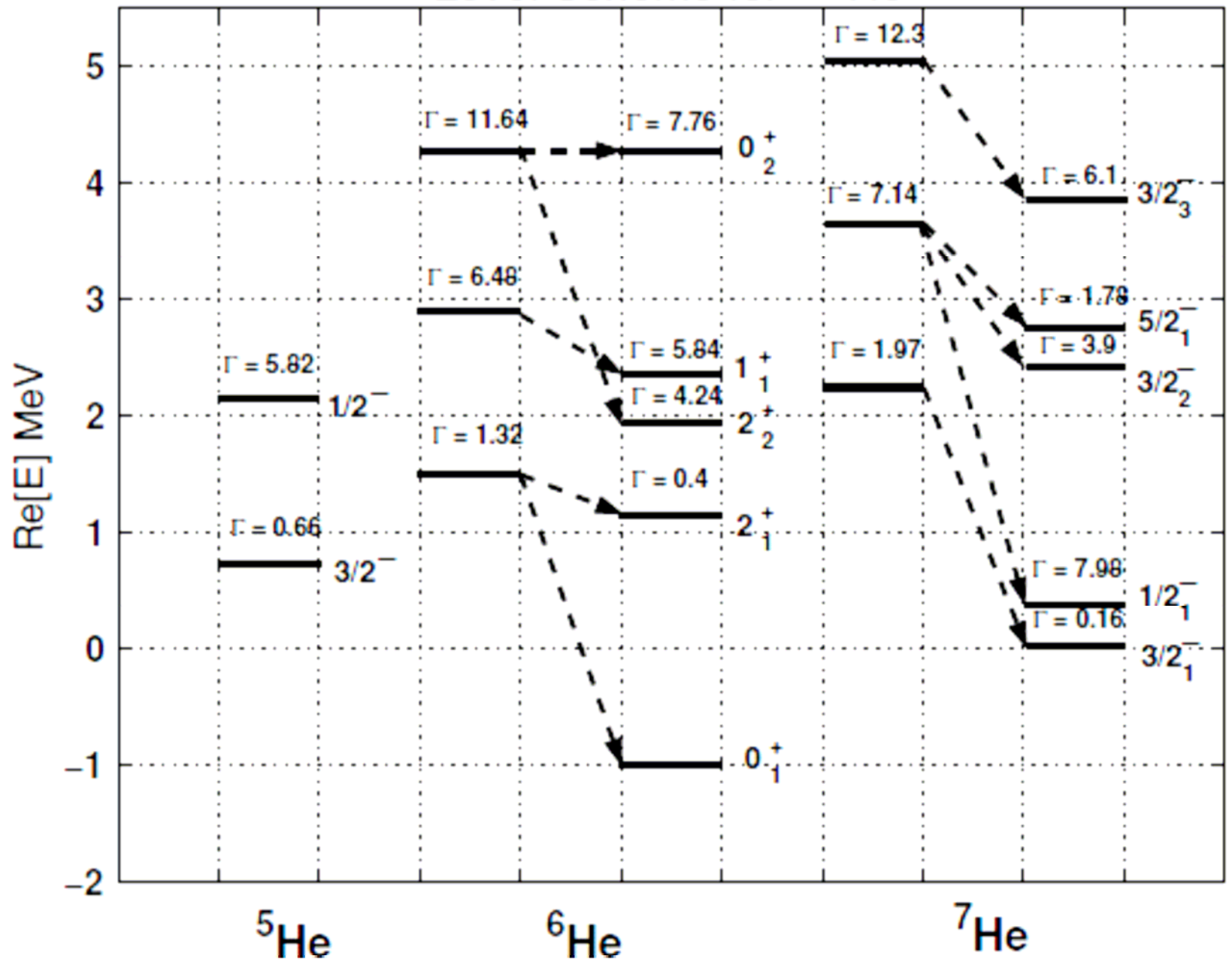
TABLE II. Single-particle neutron states in ^{78}Ni evaluated with the Woods-Saxon potential given in Table I. The complex energies are in MeV. The column labeled WS1 corresponds to $V_0 = 40$ MeV, and WS2 to $V_0 = 37$ MeV. The hole states $0g_{9/2}$ are given to show the magnitude of the gap corresponding to the magic number $N = 50$.

State	WS1	WS2
$0g_{9/2}$	(-4.398,0)	(-2.587,0)
$1d_{5/2}$	(-0.800,0)	(0.294,-0.018)
$2s_{1/2}$	(-0.295,0)	-----
$1d_{3/2}$	(1.325,-0.479)	(1.905,-1.241)
$0h_{11/2}$	(3.296,-0.013)	(4.681,-0.069)
$1f_{7/2}$	(3.937,-1.796)	(4.455,-2.851)
$0g_{7/2}$	(4.200,-0.167)	(5.799,-0.506)

TABLE VIII. Single-particle proton states in ^{100}Sn evaluated with the Woods-Saxon potential given in Table I. The complex energies are in MeV.

State	Energy
$1d_{5/2}$	(2.583,-0.000)
$2s_{1/2}$	(4.007,-0.004)
$0g_{7/2}$	(4.469,-0.000)
$1d_{3/2}$	(4.917,-0.004)
$0h_{11/2}$	(7.559,-0.001)
$1f_{7/2}$	(9.710,-0.424)
$0i_{13/2}$	(16.361,-0.210)

Level Scheme for ^{57}He



Comparison between GSM (Michel) and COSM (Masui)

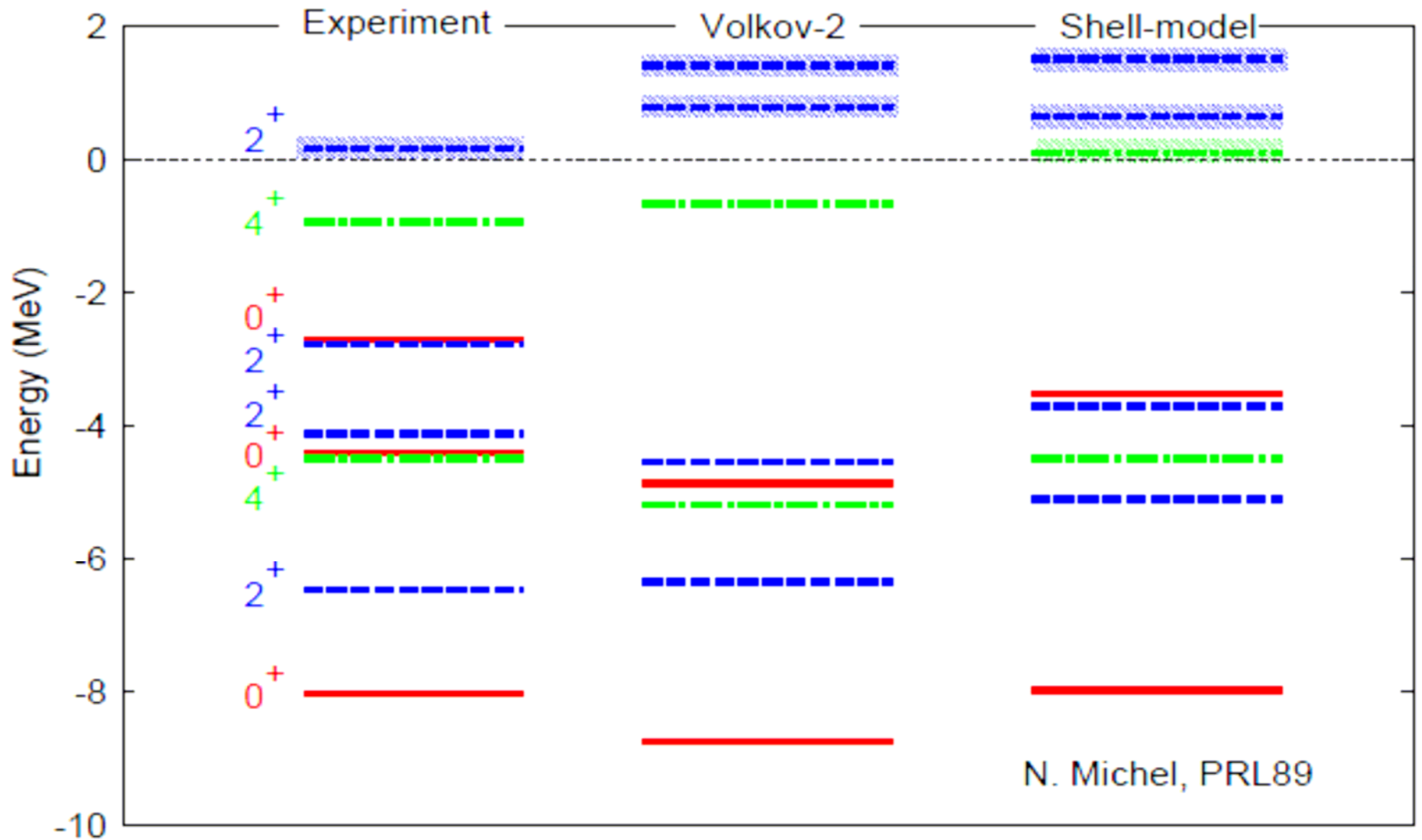


Table 4: Contribution of the poles and continua for the ^{18}O case.

		$\theta = 0$ (deg.)	$\theta = 10$ (deg.)		GSM	
Poles	$(d_{5/2})^2$	0.830	0.830	$-i2.06 \times 10^{-6}$	0.872	$+i1.15 \times 10^{-4}$
	$(s_{1/2})^2$	9.59×10^{-2}	9.59×10^{-2}	$-i1.11 \times 10^{-7}$	4.4×10^{-2}	$-i5.97 \times 10^{-6}$
	$(d_{3/2})^2$	—	2.83×10^{-2}	$-i4.55 \times 10^{-3}$	2.8×10^{-2}	$-i6.62 \times 10^{-3}$
sum		0.926	0.954	$-i4.52 \times 10^{-3}$	0.944	$-i6.61 \times 10^{-3}$
Continua	L(1)	1.06×10^{-2}	1.97×10^{-2}	$+i3.72 \times 10^{-3}$	4.2×10^{-2}	$+i4.71 \times 10^{-3}$
	L(2)	6.33×10^{-2}	2.58×10^{-2}	$+i8.05 \times 10^{-4}$	1.5×10^{-2}	$+i1.80 \times 10^{-3}$
sum		7.38×10^{-2}	4.55×10^{-2}	$+i4.53 \times 10^{-3}$	5.7×10^{-2}	$+i6.51 \times 10^{-3}$
Total		1.00	1.00	$+i4.31 \times 10^{-6}$	1.01	$-i0.10$

Table 5: Contribution of the poles and continua for the ^6He case.

	$\theta = 35$ (deg.)		GSM [3]
$(p_{3/2})^2$	1.21	$-i0.65$	$0.891 - i0.811$
$(p_{1/2})^2$	1.53	$+i0.16$	$0.004 - i0.079$
$(d_{5/2})^2$	-5.17×10^{-2}	$-i0.11$	—
$(d_{3/2})^2$	-1.92	$+i3.92$	—
$(f_{7/2})^2$	-0.75	$+i0.35$	—
sum	2.10×10^{-2}	$+i3.68$	$0.895 - i0.890$
L(1)	2.27	$-i9.20$	$0.255 + i0.861$
L(2)	-1.29	$+i5.48$	$-0.150 + i0.029$
sum	0.974	$-i3.71$	$0.105 + i0.890$
Total	0.995	$+i3.41 \times 10^{-2}$	1.00

Table 6: Contribution of poles and continuum for $d_{5/2}$.

	^{18}O	^{19}O	^{20}O
pole	0.830	0.868	0.782
L(1)	3.96×10^{-3}	5.69×10^{-3}	9.45×10^{-3}
L(2)	6.02×10^{-4}	2.37×10^{-4}	3.17×10^{-4}
L(3)	—	1.53×10^{-5}	2.28×10^{-6}
L(4)	—	—	1.55×10^{-7}

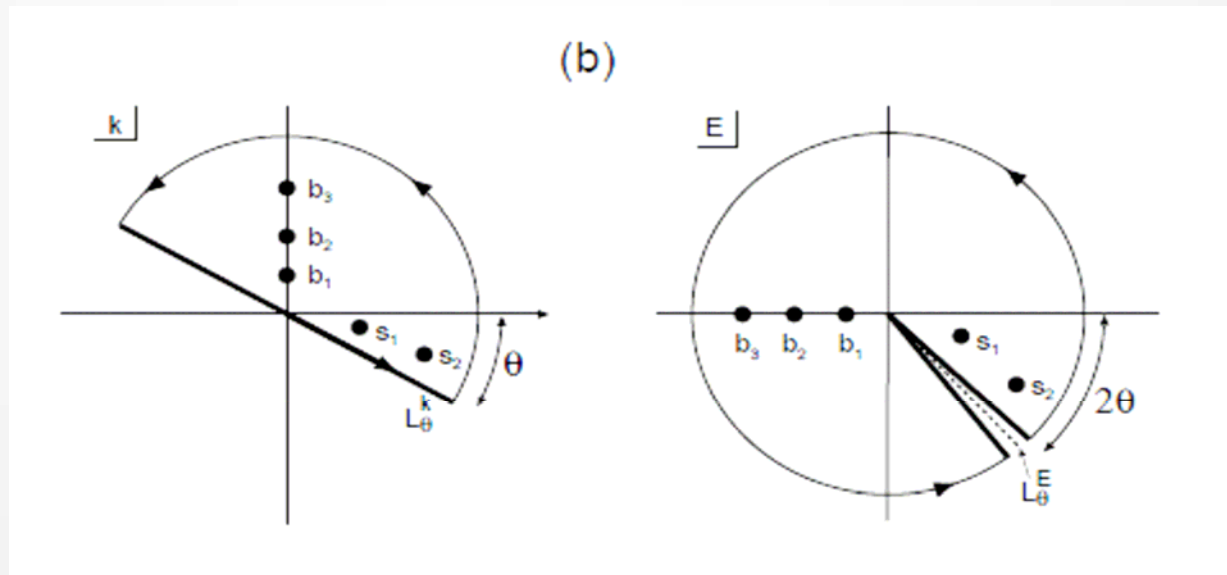
Table 7: Contribution of poles and continuum for $p_{3/2}$.

	^6He	^7He	^8He
GSM[GSM]: pole	$0.870 - i0.736$	$1.110 - i0.879$	$0.296 - i1.323$
Ours: pole	$1.21 - i0.650$	$1.43 - i1.02$	$0.252 - i1.58$
L(1)	$-0.265 + i0.675$	$-0.596 + i1.435$	$1.60 + i1.52$
L(2)	$-0.0222 - i0.0298$	$-0.0137 - i0.437$	$-1.02 + i0.235$
L(3)	—	$0.0068 + i0.0390$	$0.0682 - i0.187$

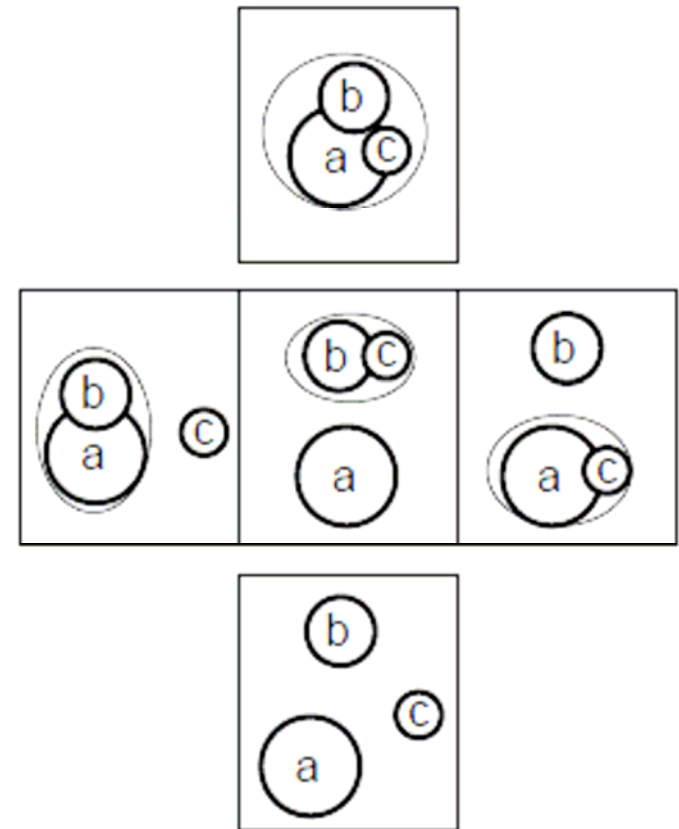
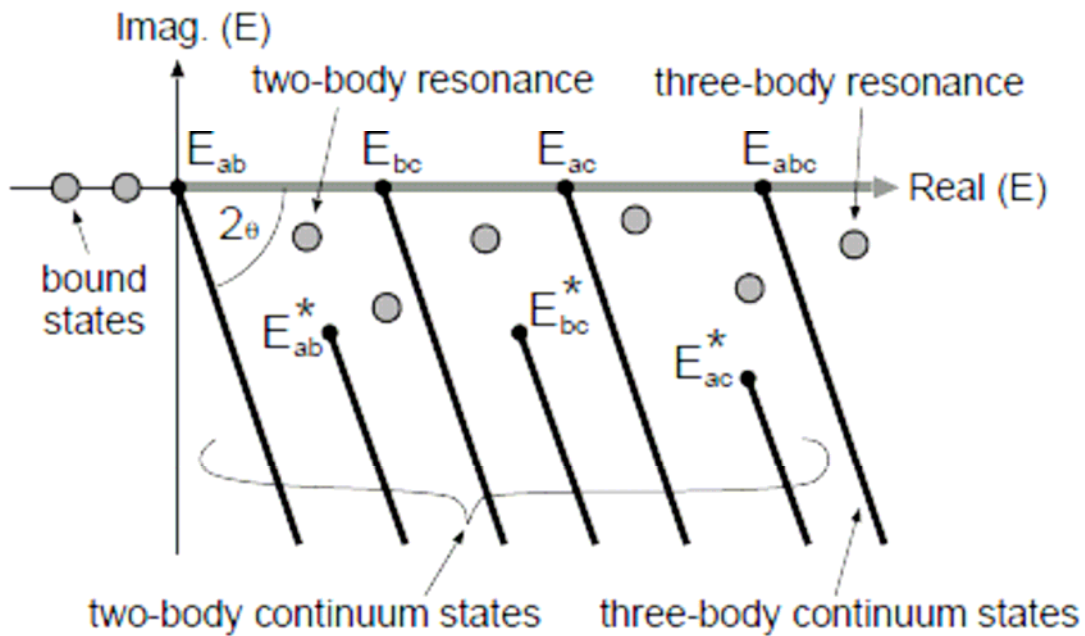
Complex Scaling Method and Gamow Shell Model

1. Contour
2. Threshold of subsystems
3. Single particle wave functions
4. Dcretization

1. Contour



2. Threshold of subsystems



3. Single particle wave functions

The Gaussian basis functions are defined by

$$\phi_{lJ}^{b_i}(\mathbf{r}) = \frac{u_l(r, b_i)}{r} \left[Y_l(\hat{\mathbf{r}}) \chi_{1/2} \right]_J, \quad (i = 1 \sim N),$$

$$u_l(r, b_i) = \sqrt{\frac{2}{\Gamma(l + \frac{3}{2}) b_i^{2l+3}}} r^{l+1} \exp\left(-\frac{r^2}{2b_i^2}\right).$$

The size parameters b_i are determined by a geometrical progression of the form $b_i = b_0 \gamma^{i-1}$ with the first term b_0 and the common ratio γ chosen so as to obtain a high numerical precision.

Ref: E. Hiyama, Y. Kino and M. Kamimura, Prog. Part. Nucl. Phys. 51, 223 (2003).

4. Dcretization

(R.Suzuki, T.Myo and K.Kato;

Prog. Theor. Phys. 113 (2005),1273-1286.)

Definition of LD: $\rho(E) = \sum \delta(E - E_i)$

$$\rho(E) = -\frac{1}{\pi} \text{Im} \left[\text{Tr} \left\{ \frac{\mathbf{1}}{E - H + i\varepsilon} \right\} \right]$$

$$= -\frac{1}{\pi} \text{Im} \left[\sum_{n_B}^{N_B} \frac{1}{E - E_{n_B}^B} + \sum_{n_R}^{N_B^\theta} \frac{1}{E - E_{n_R}^R} + \int_{L_\theta} dE^C \frac{1}{E - E^C} \right]$$

Resonance: $E_{n_R}^R = E_{n_R}^R - i \frac{\Gamma_{n_R}}{2}$ Continuum: $E^C = \varepsilon_R - i\varepsilon_I$

$$= \sum_{n_B}^{N_B} \delta(E - E_{n_B}^B) + \frac{1}{\pi} \sum_{n_R}^{N_R^\theta} \frac{\Gamma_{n_R} / 2}{(E - E_{n_R}^R)^2 + \Gamma_{n_R}^2 / 4} + \frac{1}{\pi} \int_{L_\theta} dE^C \frac{\varepsilon_I}{(E - \varepsilon_R)^2 + \varepsilon_I^2}$$

$$\begin{aligned}
\Delta(E) &= \rho^\theta(E) - \rho_0^\theta(E) \\
&= -\frac{1}{\pi} \text{Im} \left[\text{Tr} \left\{ G^\theta(E) - G_0^\theta(E) \right\} \right] \\
&= -\frac{1}{\pi} \text{Im} \left[\text{Tr} \left\{ \frac{1}{E - H_\theta} - \frac{1}{E - H_0^\theta} \right\} \right]
\end{aligned}$$

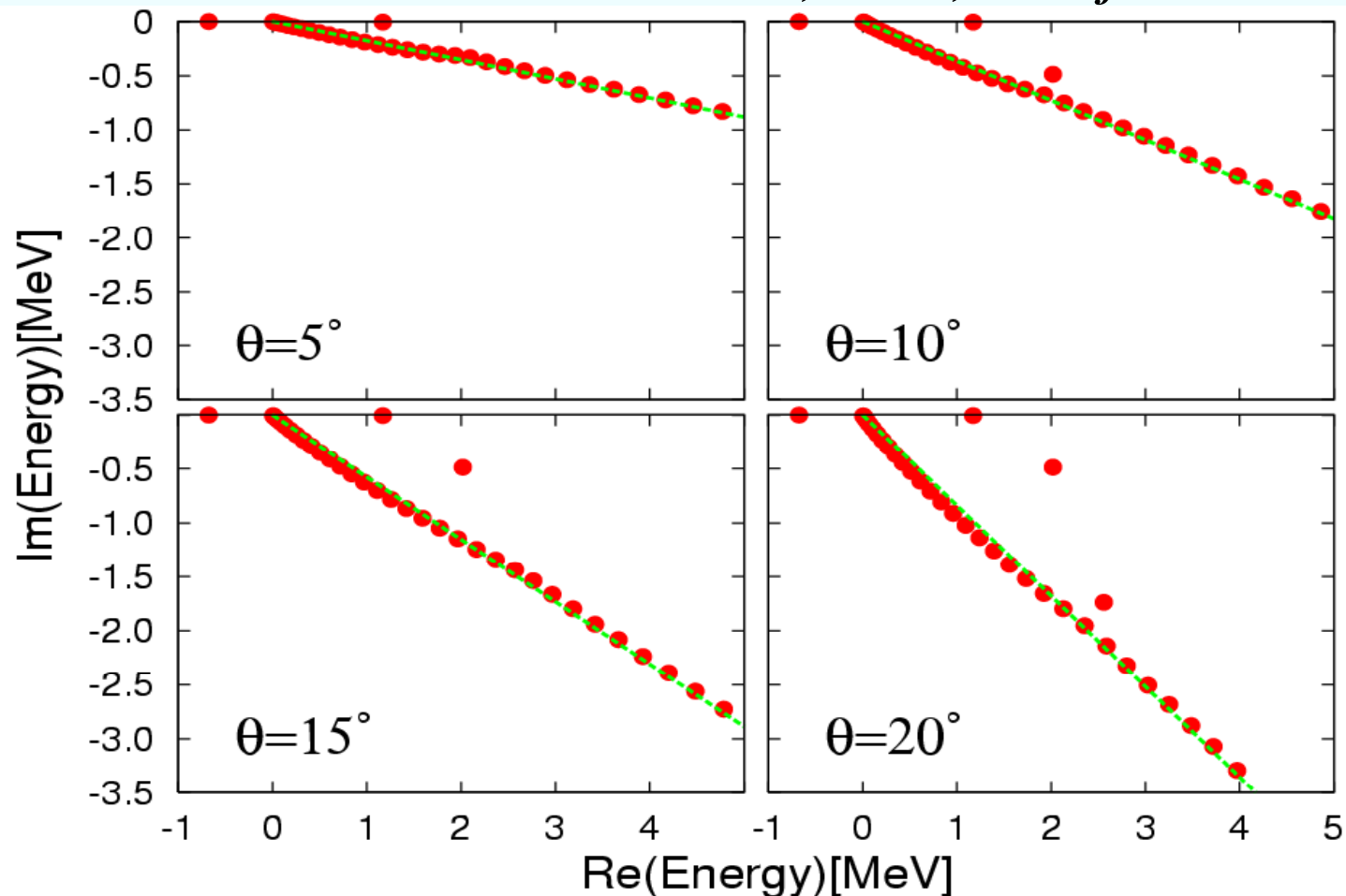
$$\begin{aligned}
\Delta^M(E) &= -\frac{1}{\pi} \text{Im} \left[\sum_B \frac{1}{E - e_B} + \sum_R^{N_\theta} \frac{1}{E - e_R^\theta} + \sum_C \frac{1}{E - e_C^\theta} - \sum_j^M \frac{1}{E - \epsilon_j^0(\theta)} \right] \\
&= g_{M,B}(E) + g_{M,R}^\theta(E) + g_{M,C}^\theta(E)
\end{aligned}$$

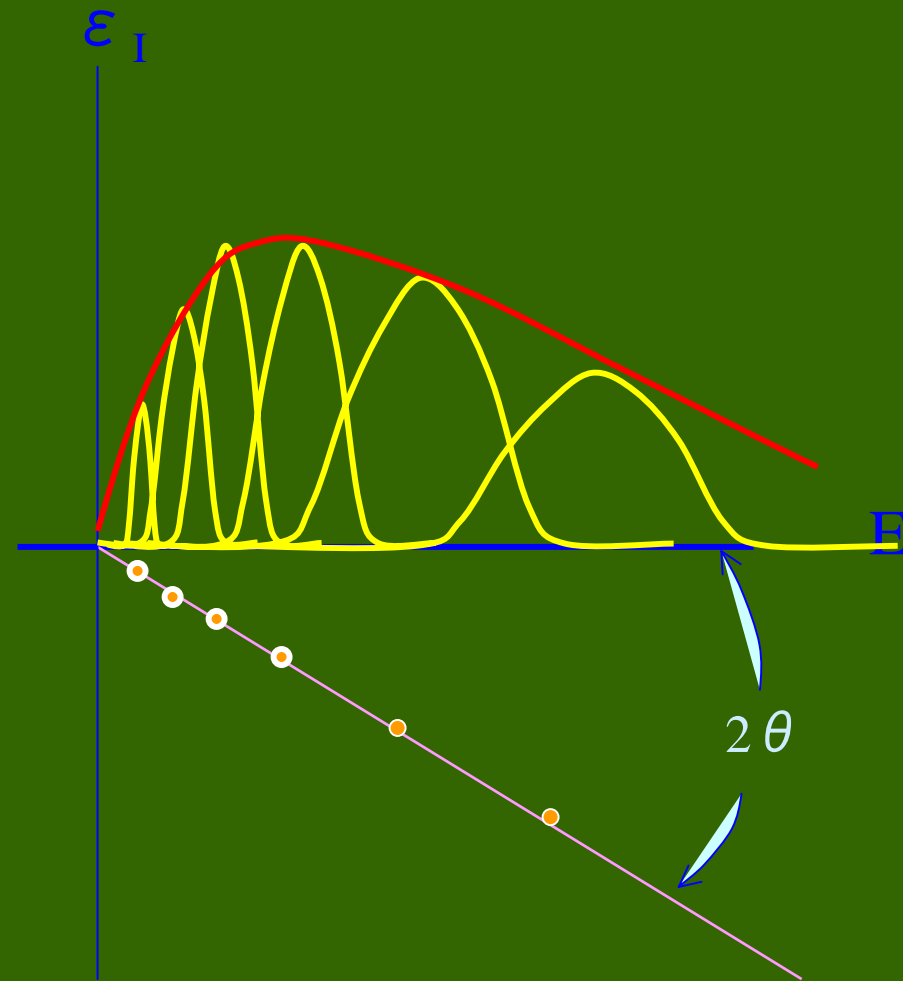
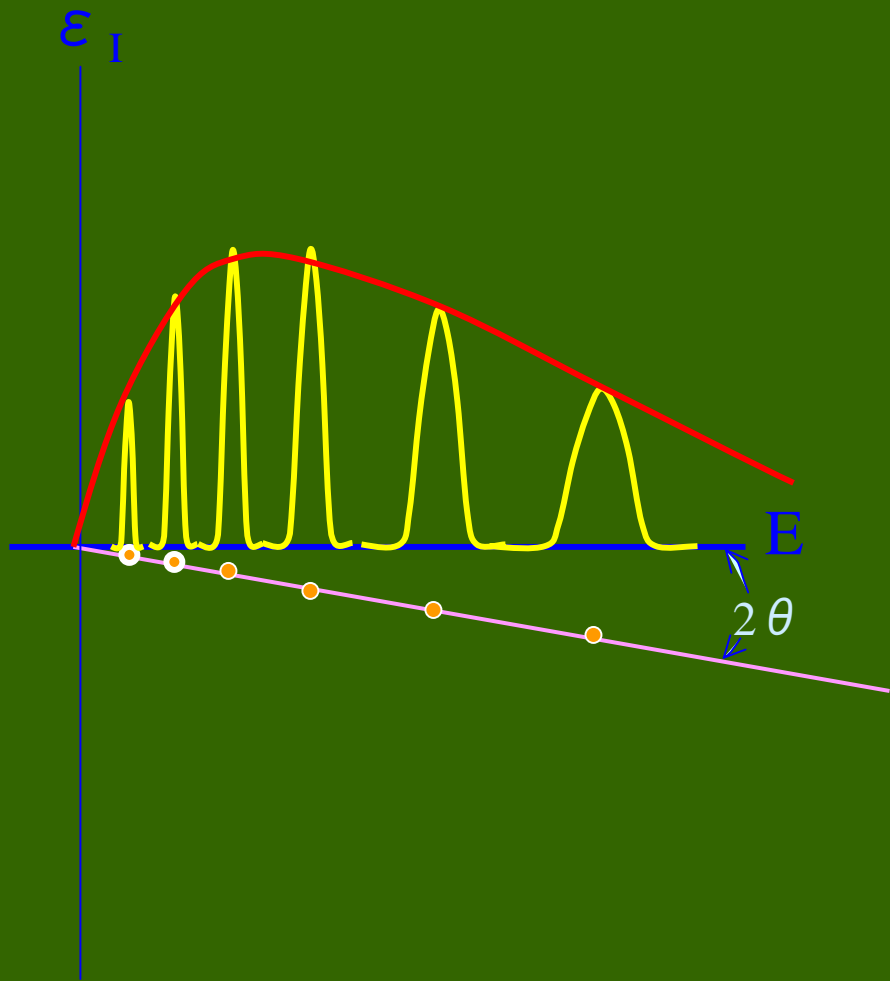
Schematic potential problem

$$H = T + V, \quad V(r) = -8.0e^{-0.16r^2} + 4.0e^{-0.04r^2}$$

[ref: A. Csoto, et al, Phys. Rev. A41(1990)3469]

Energy eigenvalue distribution of 1^- state
Harmonic Oscillator basis; $N=50, b=2.5\text{fm}$

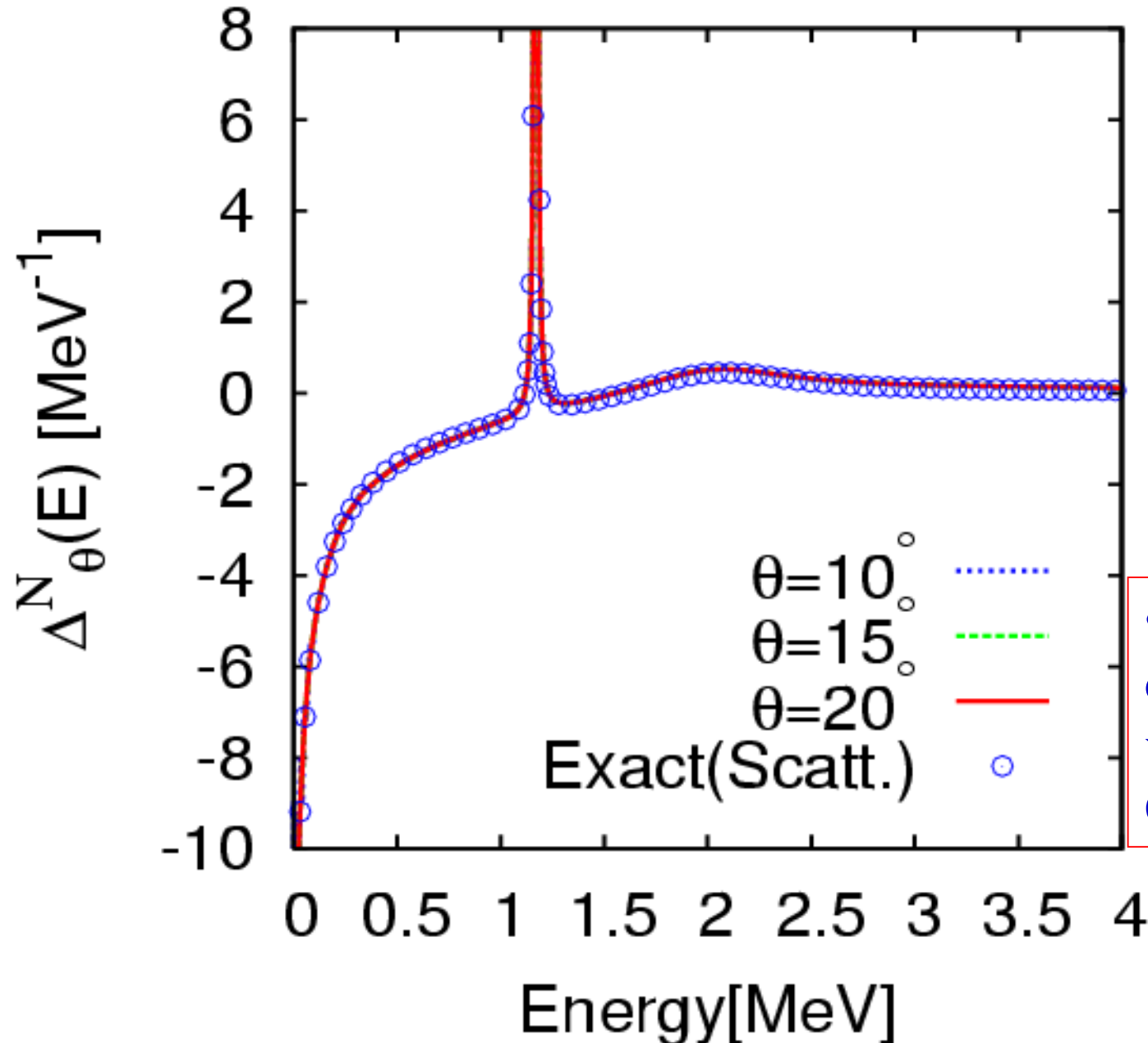




This is a kind of “wavelets” to transform analog data to digital ones.

(I. Daubechies, “*Ten Lectures on Wavelets*” Society for Industrial and Applied Mathematics, Philadelphia, PA, 1992)

$\Delta_{\theta}^N(E)$: *Gaussian basis; $N=30$, $b_0=0.2\text{fm}$, $\gamma=1.2$*



• Discretization of continuum states is very successful in CSM.